Vol 18 No 1, January 2009
1674-1056/2009/18(01)/0016-07

Chinese Physics B

© 2009 Chin. Phys. Soc.
and IOP Publishing Ltd

The influences of thickness of spacing layer and the elastic anisotropy on the strain fields and band edges of InAs/GaAs conical shaped quantum dots*

Liu Yu-Min(刘玉敏), Yu Zhong-Yuan(俞重远), and Ren Xiao-Min(任晓敏)

Institute of Optical Communication and Optoelectronic, Beijing University of Posts and Telecommunications, Beijing 100876, *China*

Key Laboratory of Optical Communication and Lightwave Technologies, Ministry of Education

(Beijing University of Posts and Telecommunications), Beijing 100876, *China*

(Received 13 November 2007; revised manuscript received 6 June 2008)

Based on the continuum elastic theory, this paper presents a finite element analysis to investigate the influences of elastic anisotropy and thickness of spacing layer on the strain field distribution and band edges (both conduction band and valence band) of the InAs/GaAs conical shaped quantum dots. To illustrate these effects, we give detailed comparisons with the circumstances of isolated and stacking quantum dot for both anisotropic and isotropic elastic characteristics. The results show that, in realistic materials design and theoretical predication performances of the optoelectronic devices, both the elastic anisotropy and thickness of the spacing layer of stacked quantum dot should be taken into consideration.

Keywords: quantum dot, strain, electronic structure
PACC: 0365, 2110D

1. Introduction

Quantum dots (QDs) have attracted great attention due to their atom-like characteristics and thus potential application in fabricating a wide variety of novel optoelectronic and microelectronic devices.[1−2] With the development of material growth technique, especially the advanced molecular-beam epitaxy and metal organic chemical vapour deposition technologies, self-organized QDs can be grown layer by layer to form ordered array via the Stranski–Krastanow (S–K) growth style.[3] In S–K growth style, the two-dimensional wetting layer will first appear on the substrate, when the thickness of the wetting layer reaches the so-called 'critical thickness',[4] the three-dimensional island transition will exhibit via lattice relaxation. It has been known that the lattice mismatch between the QDs and the substrate is the main driving force in S–K growth mode. The elastic strain field produced by the quantum dot can strongly influence the order of the next sheet of the QDs by the long-range interaction. Based on the deformation theory, the strain semiconductor will substantially modify the electronic band offset and further affect the performance of the devices. So it is necessary to study the strain in and around the QDs to control the ordered QDs array and tuning the device's functions via the strain engineering.[5,6]

The elastic strain fields have been extensively evaluated by using different methods such as atomic potential approach, analytical continuum approach, and finite element method. The atomic potential methods are based on few-body (generally three-body) potential between the atoms such as the Keating potential, Stillinger–Weber (S–W) potential,[7] and Tersoff potential.[8] The calculations based on atomic potentials require a large amount of atomic information, which leads to high computation resource. So this method is only limited to a single isolated quantum dot, which contains atoms fewer than 10000. The continuum approaches assume that the QDs are inclusions of an infinite matrix,[9] however it is impossible for realistic a QD array to be infinite. The numerical finite element method is powerful and can be easily used to simulate the realistic quantum dot structure.

Literature including related calculations about the elastic fields of QDs often follow simplified assumptions, for example, dealing with a single iso-

*Project supported by the National Basic Research Program of China (Grant No 2003CB314901), the National Natural Science Foundation of China (Grant No 60644004), and the High School Innovation and Introducing Talent Project of China (Grant No B07005).

lated QD, and ignoring the strain coupling between the QDs,[7] assuming an infinite matrix, but with the QDs buried under free surfaces,[9] without considering the wetting layer,[10] an isotropic elastic assumption and taking the same elastic constants for both the QDs and the substrate,[11] and so on. Recently a few works have begun to study some of these effects on strain field distribution and predicate the effects on the ordering of the post-growth of QD array.[12,13] As far as we know, little work has been done on the combination effects of the elastic anisotropy, the spacing thickness and the wetting layer on both the strain distribution and the band offset of the QDs. In this work, we use the finite element method to investigate the strain distributions of InAs/GaAs materials for both isolated QD and stacking QDs. Both the isotropic and anisotropic elastic characteristics are taken into consideration. Based on the strain field, the band offsets are numerically evaluated by the eight-band $\boldsymbol{K}\cdot\boldsymbol{P}$ theory.

2. Physical model

The finite element calculations are especially useful in processing complicated strain problems such as the strain distribution of complex shaped QDs.[12,13] But for a QD stacking array, a complete three-dimensional strain solver will require expensive computational cost. It has been checked that the time consuming three-dimensional calculations (with the other island shape) give no significantly different results.[11] So here we adopt the axial symmetry (conical islands) model.

The details of the numerical analysis can be found in previously published works.[14–16] In the following, we only give some short descriptions. In our model, the QD is grown along the (001) direction, which is defined as the z-axis of the coordinate system. For the axis-symmetry mode, the cylindrical coordinate system is taken into consideration, where the horizontal axis is the radial direction. The geometries of both the isolated QD and multi-layer QDs (which have been meshed) are shown in Fig.1. From the previews works, it has been found that the long-range strain produced by the QD cannot provide obvious influence in the substrate and cap layer when the distance of the capping layer and substrate is larger than three times height of the QD. So in this work, seven-layer stacking QDs model is enough to simulate the strain coupling effects. To simulate the isolated QD in numerical analysis, we assume that both the substrate and the cap layer are thick enough. In this work, the thickness of the substrate is assumed to be 60 nm (for strain calculations, when the thickness is large than 60 nm, no different results can be obtained). The distance from left-boundary to the right-boundary of the geometry is 30 nm, so the strain coupling for the transverse aligned QD can be ignored. The height of the QD is 4.5 nm, the thickness of the wetting layer is 0.5 nm, and the thickness of the spacing layer (including the wetting layer) is 6 nm.

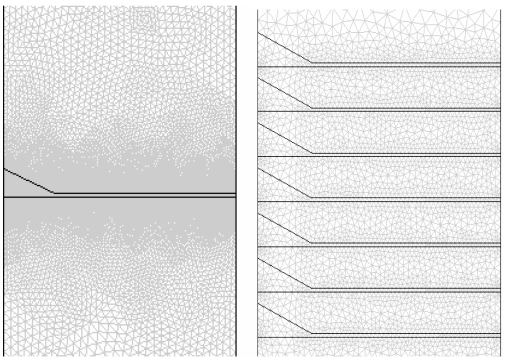


Fig.1. The geometry of the QDs used for numerical analysis. (a) Isolated QD model, and (b) the seven layer stacking QDs model.

For cubic symmetric InAs/GaAs materials, the strain and stress are determined by three independent elastic constants. It is convenient to describe the strain and stress tensors as two columns vectors, and then the relation of strain and stress can be expressed as a stiffness matrix:

$$\begin{pmatrix}\sigma_{xx}\\ \sigma_{yy}\\ \sigma_{zz}\\ \sigma_{xy}\\ \sigma_{yz}\\ \sigma_{xz}\end{pmatrix}=\begin{pmatrix}C_{11} & C_{12} & C_{12} & 0 & 0 & 0\\ C_{12} & C_{11} & C_{12} & 0 & 0 & 0\\ C_{12} & C_{12} & C_{11} & 0 & 0 & 0\\ 0 & 0 & 0 & C_{14} & 0 & 0\\ 0 & 0 & 0 & 0 & C_{14} & 0\\ 0 & 0 & 0 & 0 & 0 & C_{14}\end{pmatrix}\begin{pmatrix}\varepsilon_{xx}-\varepsilon_0\\ \varepsilon_{yy}-\varepsilon_0\\ \varepsilon_{zz}-\varepsilon_0\\ \varepsilon_{xy}\\ \varepsilon_{yz}\\ \varepsilon_{zx}\end{pmatrix}+\sigma_0. \tag{1}$$

For the isotropic assumption, only two quantities are used to simulate the strain problem which are the Young moduli and the Poisson ratios. The two quantities can be converted into a similar style just as expression (1). The anisotropic elastic constants for InAs and GaAs are taken from the Ref.[17]. The isotropic elastic constants of InAs and GaAs are taken from the Ref.[11]. In both circumstances, the elastic constants are shown in Table 1.

Table 1. The three independent elastic constants (GPa), the Young moduli (GPa) and Poisson ratios for InAs and GaAs.

	C_{11}	C_{12}	C_{44}	E	v
InAs	83.4	45.4	39.5	51.42	0.35
GaAs	118.8	53.8	59.4	86.96	0.31

In expression (1), σ_0 and ε_0 are initial stress and initial strain respectively. For the whole system, the initial stress is zero. The initial strain in the GaAs region is zero. In the InAs region the initial strain is the lattice misfit between InAs and GaAs. The lattice misfit is defined as:

$$\varepsilon_0 = \left(a_{\mathrm{GaAs}} - a_{\mathrm{InAs}}\right)/a_{\mathrm{InAs}} = -0.067, \qquad (2)$$

where a_{InAs} and a_{GaAs} are the lattice constant of InAs and GaAs respectively. In the framework of thermoelasticity, to simulate initial strain, the thermal expansion coefficient of the InAs QD and wetting layer is set to be the absolute value of lattice mismatch between InAs and GaAs, which is $0.067\,\mathrm{K}^{-1}$. The thermal expansion coefficient of GaAs is set to be zero. Then the initial strain of the system can be simulated by raising the temperature from reference temperature 0 K to the strain temperature 1 K.

There is only relative meaning for the values of the reference temperature and strain temperature. But the difference between the strain temperature and reference temperature should be 1 K. Then the initial strain can be substituted by the effect of thermal expansion process.[14−16] The thermal expansion simulation environment is easy to be realized by using the commercial finite element tools such as ANSYS, COMSOL *et al.*

The effect of the strain on the band offset can be derived from the solid deformation theory. In the framework of eight-band $\boldsymbol{K}\cdot\boldsymbol{P}$ theory, strain modified band edges are expressed as[18]

$$E_{\mathrm{c}} = E_{\mathrm{v,av}} + \frac{\Delta_0}{3} + E_{\mathrm{g}} + a_{\mathrm{c}}\varepsilon_{\mathrm{hyd}}, \qquad (3)$$

$$E_{\mathrm{hh}} = E_{\mathrm{v,av}} + \frac{\Delta_0}{3} + a_{\mathrm{v}}\varepsilon_{\mathrm{hyd}} - \frac{1}{2}b\varepsilon_{\mathrm{bi}}, \qquad (4)$$

$$E_{\mathrm{lh}} = E_{\mathrm{v,av}} - \frac{\Delta_0}{6} + a_{\mathrm{v}}\varepsilon_{\mathrm{hyd}} + \frac{1}{4}\delta E^{\mathrm{sh}} + \frac{1}{2}\sqrt{\Delta_0^2 + \Delta_0\delta E^{\mathrm{sh}} + \frac{9}{4}\left(\delta E^{\mathrm{sh}}\right)^2}, \qquad (5)$$

$$E_{\mathrm{lh}} = E_{\mathrm{v,av}} - \frac{\Delta_0}{6} + a_{\mathrm{v}}\varepsilon_{\mathrm{hyd}} + \frac{1}{4}\delta E^{\mathrm{sh}} - \frac{1}{2}\sqrt{\Delta_0^2 + \Delta_0\delta E^{\mathrm{sh}} + \frac{9}{4}\left(\delta E^{\mathrm{sh}}\right)^2}, \qquad (6)$$

where $E_{\mathrm{v,av}}$ is the unstrained average valence band edge, $\delta E^{\mathrm{sh}} = b\varepsilon_{\mathrm{bi}}$ is the band deformation related to bi-axial strain, Δ_0 is spin–orbit splitting energy, E_{g} is band gap, a_{c} and a_{v} are conduction band and valence band deformation potential respectively. The hydrostatic strain and bi-axial strain are $\varepsilon_{\mathrm{hyd}} = \varepsilon_{rr} + \varepsilon_{\phi\phi} + \varepsilon_{zz}$ and $\varepsilon_{\mathrm{bi}} = 2\varepsilon_{zz} - \varepsilon_{rr} - \varepsilon_{\phi\phi}$ respectively. The values of the parameters used in the calculations are taken from Ref.[18] and are also shown in Table 2.

Table 2. The deformation potential and band structure parameters of InAs and GaAs.

	a_{c}	a_{v}	b	$E_{\mathrm{v,av}}$	E_{g}	Δ_0
InAs	–5.08	1.00	–1.8	0.25	0.67	0.34
GaAs	–7.17	1.16	–1.7	0.00	1.519	0.38

3. Results and discussions

We first investigate the strain distributions of the isolated QD with isotropic and anisotropic elastic characteristics. Figure 2 shows the two normal strain components distributions in cylindrical coordinate system for the isolated QD. Both the isotropic and anisotropic models are presented for comparison. The ε_{zz} component represents the strain along the [001] direction, and ε_{rr} represents [100] or [010] direction in the corresponding three-dimensional calculations. From the contour plots, it is easy to found that the ε_{rr} component is more sensitive to the anisotropy in comparison with the ε_{zz}. This is especially obvious in the InAs QD region. In the anisotropic model, for both strain components, the strain equal-value belts tend to extend along the [001] direction. While in the isotropic model, for both strain components, it is obvious that the strain equal-value belts extend along the radial direction. It should be further noticed that the ε_{zz} strain in and outside of the QD exhibits similar distributions, especially in the strain concentration locations, such as the corner between the QD and wetting layer, and the matrix part near to the

QD apex and base. We can see in these regions that the anisotropy will lead to a stronger long-range elastic interaction, which is very important for the orderly QD array via strain engineering.[12] This trend is more obvious for the ε_{rr} components. So the anisotropic model means strong lattice relaxation and reduction of strain energy. In Fig.3, the strain contour plots of stacking QDs are shown. Just as expected, the strain components show the same trend as the isolated QD. However, the trend seems no more obvious than that of the isolated conditions. This may be attributed to the stronger elastic coupling of the vertical aligned QDs, which cancel or trail off the anisotropic effects. The strain coupling effects can be seen by quantitative comparison between Fig.2 and Fig.3. It is easy to notice that the influences of the strain equal-value belt distributions, due to the strain coupling of the vertical QDs, are obvious. Figure 4 shows the detailed strain information along the central axis of the isolation and stacking QDs for the isotropic model.

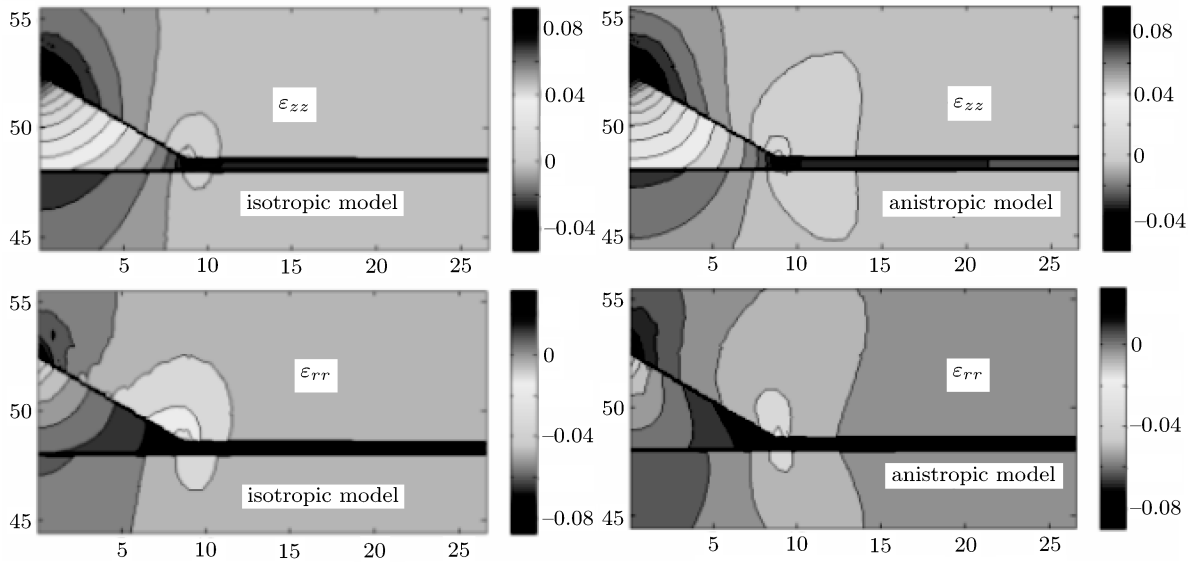


Fig.2. The strain contour plots of an isolated QD with isotropic and anisotropic model.

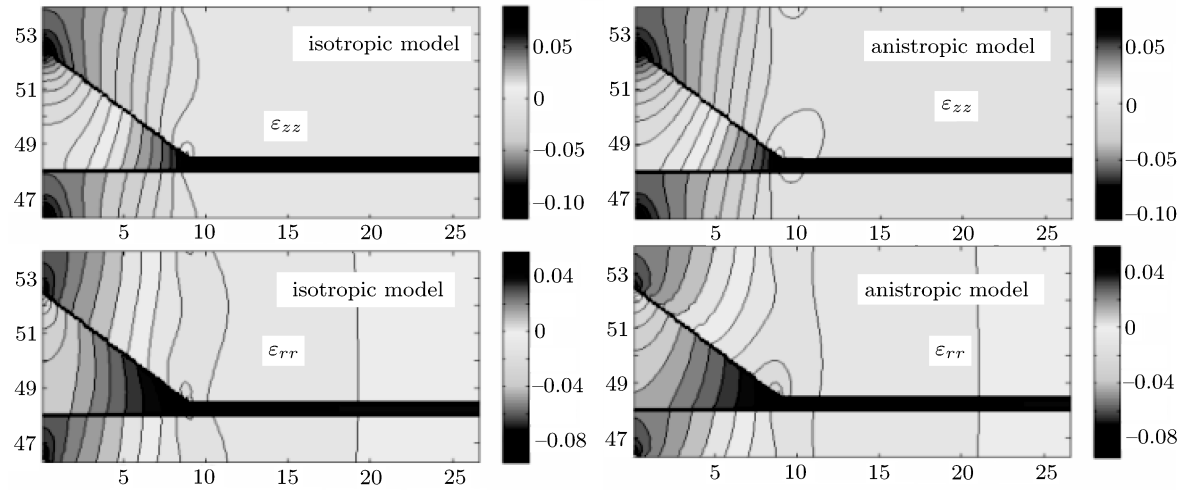


Fig.3. The strain contour plots of stacking QDs with isotropic and anisotropic model (only the strains of mid-layer QD are shown).

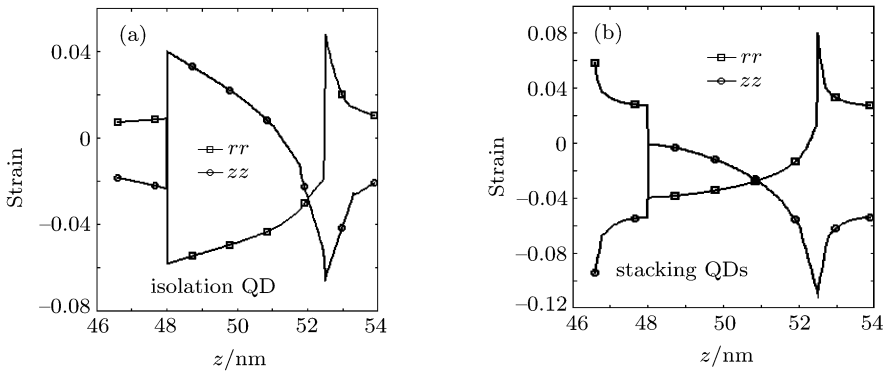


Fig.4. Isotropic model calculated strain distribution cut through the central axis direction of the QD. (a) The isolation QD, and (b) the mid-layer QD of the stacking QDs, and the legend rr and zz represent the ε_{rr} and ε_{zz} strain component respectively.

It can be seen from Figs.3 and 4 that both the strain coupling and the anisotropic elastic characteristics present a noticeable change to the strain distributions. Especially, from Fig.4, the strain coupling leads to obvious strain reduction in the QD region, and strain enhancement in the barrier region.

The effects of elastic anisotropy on the elastic fields have been study by Pei *et al*,[19] but in that work the material parameters are given arbitrarily, and the studied QD is lens-shaped. The influences of anisotropy on the elastic fields (Fig.3 of the literature) qualitatively agree with our calculated results of InAs/GaAs conical shaped QD.

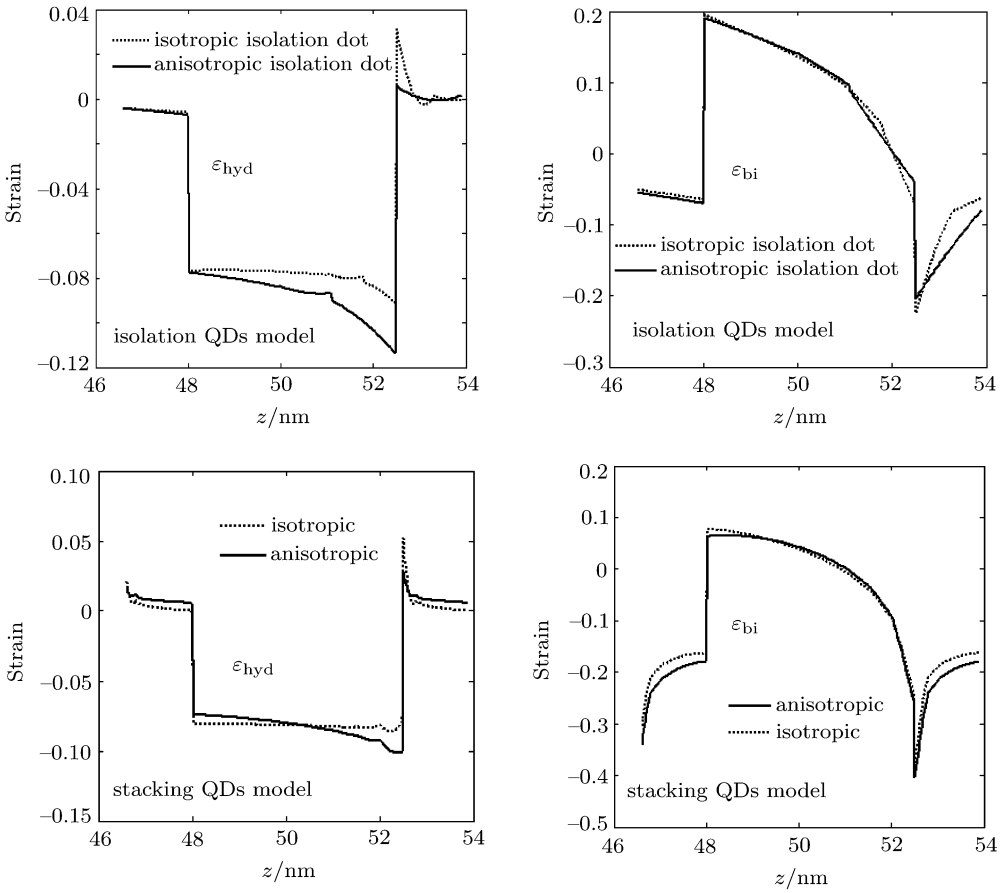


Fig.5. The hydrostatic strain and bi-axial strain distribution cut through the central axis of the QD. Both the isotropic and anisotropic elastic model are shown. The up parts are the isolation QD model, the bottom parts are the stacking QDs model (only the strains of the mid-layer QD are shown).

In the following, we will give some investigations about influences of the strain distributions with the strain coupling and anisotropic elastic characteristics on the band edge alignment. From expressions (3)–(6), the band edge modifications are mainly dependent on the hydrostatic strain and bi-axial strain. Figure 5 shows the hydrostatic and bi-axial strain components of both the isolation and stacking QDs including the isotropic and anisotropic model. It is easy to see that the bi-axial strain is not sensitive to the anisotropic elastic characteristics for both the isolated and stacking QDs. However, the hydrostatic strain is very sensitive to the anisotropic model, especially near the apex region of the isolation QD. The isotropic model underestimates the hydrostatic strain value by about 25%. Compared with the isolation QD, the stacking QDs have reduced hydrostatic strain amplitude in the QD region, and enhanced amplitude in the barrier region. The isotropic model overestimates the hydrostatic strain value near the base of the QD, but underestimates it near the QD apex. In the stacking QDs, the strain coupling effects produce a big variation in amplitude for the bi-axial strain components. The amplitude of the bi-axial strain is reduced about 50% in the QD region, while enhanced in the barrier region to about three times that of the isolation QD.

Based on the hydrostatic strain, bi-axial strain and the band structure parameters in Table 2, we can estimate all the band edge information in the centre of the Brillouin zone. Figure 6 shows the strain modified band structure, both the isotropic and anisotropic models are shown, where E_{c0}, E_{v0} and E_{sp} are unstrained band edge for conduction band, valence band, and spin splitting band respectively. E_{ciso}, E_{caniso} are the modified conduction band edge calculated by using the isotropic and anisotropic model. E_{hhiso}, $E_{hhaniso}$, E_{lhiso}, $E_{lhaniso}$, E_{spiso}, and $E_{spaniso}$ are the heavy hole, light hole and spin splitting band edges. The subscripts iso and aniso indicate that the results are calculated by using the isotropic and anisotropic model respectively.

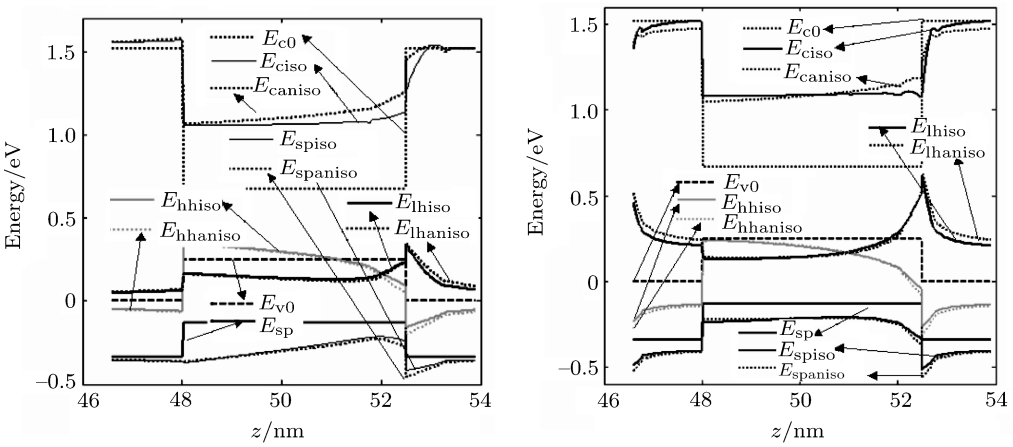


Fig.6. The strain modified band structures cut through the central axis of the QD. (a) The isolation QD, (b) the stacking QDs (only the band structures of the mid-layer QD are shown).

It is easy to find that, for both isolation and stacking QDs, the conduction band in the QD region are flatter for the isotropic model than the anisotropic model. The largest variation can be found near the apex of the QD. However, the heavy hole, light hole, and spin splitting band are not sensitive to whether the choice is the elastic isotropic model or the anisotropic model.

To quantitatively discuss the strain coupling effects on the band edge, we show the strain modified band structure of the isolation QD and the stacking QD in Fig.7. Both isotropic and anisotropic model are respectively employed to the isolation QD and stacking QDs. As can be seen, all the band edges suffer an evident shift due to the strain coupling from the other layer of QDs. For the conduction band, in the barrier region, the amplitude is decreased, but in the QD region, the effect is opposite. The heavy hole and light hole band edges undergo a reverse change, under the influence of strain coupling. The heavy hole downward shifts its largest amplitude about 40% in the QD and barrier regions, while the light hole band edge upward shifts its largest amplitude about 45% in the barrier region. There is no obvious change can be

found in the QD region. Generally, the ground state of the valence band is the heavy hole like state, so it is evident that the strain coupling will lead to the blue shift of the photoluminescence peak.

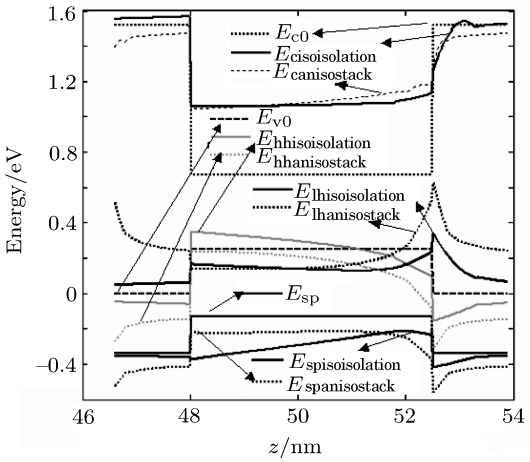


Fig.7. The strain modified band structure for isolation QD and stacking QD.

Although no direct experimental data can prove the calculated results above, the photoluminescence of low dimensional semiconductor structure under pressure has been studied extensively in the literature.[20,21] In this literature, the stress and strain originally form the press, but the influence to the peak of photoluminescence is mainly due to the strain in the microscopic region of the QD.

4. Conclusions

Based on the simulations about the strain fields and band edge calculations, we find that the following conclusions are evident. First, the anisotropic model reflects that the band gap widening effect is mainly due to the hydrostatic strain, which leads to the upward shift of conduction band edge near the QD apex, but the isotropic model underestimates this effect. Second, the strain coupling effects greatly enlarge the band gap due to the changed bi-axial strain, which leads to downward shifting of its band edge for the heavy hole. So it can be concluded that both the elastic anisotropic characteristics and the strain coupling effects should be taken into consideration for either evaluation of the strain field or prediction of the band structure of QDs material in device design.[22−24]

References

[1] Weng W C and Stephan W K 2005 *IEEE J. Quantum Electron.* **41** 495

[2] Vadim V 2006 *J. Appl. Phys.* **100** 076101

[3] Zubia D, Zaidi S H, Hersee S D and Brueck S R J 2000 *J. Vacuum Sci. Technol.* B **18** 3514

[4] Melnik R V N and Willatzen M 2004 *Nanotechnology* **15** 1

[5] Seravalli L, Minelli M, P Frigeri and Franchi S 2007 *J. Appl. Phys.* **101** 024313

[6] Liu Y M, Yu Z Y and Ren X M 2008 *Chin. Phys. Lett.* **25** 1850

[7] Kikuchi Y, Sugii H and Shintani K 2001 *J. Appl. Phys.* **89** 1191

[8] Migliorato M A, Cullis A G, Fearn M and Jefferson J H 2002 *Phys. Rev.* B **65** 115316

[9] Liu Y M, Yu Z Y and Ren X M 2008 *Chin. Phys.* B **17** 3471

[10] Ponchet A, Lacombe D, Durand L, Alquier D and Cardonna J M 1998 *Appl. Phys. Lett.* **72** 2984

[11] Benabbas T Androussi Y and Lefebvre A 1999 *J. Appl. Phys.* **86** 1945

[12] Gunther Springholz 2005 *C. R. Physique* **6** 89

[13] Song Y X, Yu Z Y and Liu Y M 2008 *Acta Phys. Sin.* **57** 2399 (in Chinese)

[14] Liu Y M, Yu Z Y and Huang Y Z 2006 *Int. J. Mod. Phys.* B **20** 4899

[15] Liu Y M, Yu Z Y, Huang Y Z and Yang H B 2006 *Acta Phys. Sin.* **55** 5023 (in Chinese)

[16] Liu Y M, Yu Z Y and Huang Y Z 2007 *J. University Sci. Technol. Beijing* **14** 477

[17] Pan E and Zhu R 2006 *J. Appl. Phys.* **100** 013527

[18] Shin H Kim J B and Yoo Y H 2006 *J. Appl. Phys.* **99** 023521

[19] Pei Q X, Lu C and Wang Y Y 2003 *Phys. Rev.* B **93** 1487

[20] Li G H, Chen Y, Fang Z L, Ma B S, Su F H and Ding K 2005 *J. Infrared Millim. Waves* **24** 174 (in Chinese)

[21] Ma B S, Wang X D, Luo J W, Su F H, Fang Z L, Ding K, Niu Z C and Li G H 2005 *J. Infrared Millim. Waves* **24** 207 (in Chinese)

[22] Jiao R Z, Feng C X and Ma H Q 2008 *Acta Phys. Sin.* **57** 1352 (in Chinese)

[23] Liu Y M, Yu Z Y and Yang H B 2005 *Opt. Commun.* **246** 367

[24] Jiao R Z and Feng C X 2008 *Acta Phys. Sin.* **57** 685 (in Chinese)